*Articles*

*Anal. Chem.* **1996,** *68,* 2289−2295

# Intrinsic Sol−Gel Clad Fiber-Optic Sensors with Time-Resolved Detection

Clarice A. Browne, Darcy H. Tarrant, Marta S. Olteanu, Joseph W. Mullens, and Eric L. Chronister*

*Department of Chemistry, University of California, Riverside, California 92521*

**Sol−gel clad fiber-optic waveguides are investigated as intrinsic distributed fiber-optic chemical sensors. The porous sol−gel cladding allows diffusion of analytes into the evanescent field region close to the fiber-optic core. Pulsed optical excitation (0.5 ns) and time-resolved emission detection can be used to simultaneously monitor several multiplexed sensor clad regions along a single optical fiber. Time-resolved detection is also demonstrated as a means of resolving both the spatial location and the fluorescence kinetics of intrinsic sensor chromophores along the fiber-optic waveguide. Narrow band excitation and spectrally resolved emission provide additional experimental means for discriminating between specific sensor clad regions. A fluorescein-doped silica xerogel clad pH sensor and an undoped aluminosilica xerogel clad quinone sensor are demonstrated as intrinsic sol−gel clad fiber-optic sensors.**

Fiber-optic chemical sensors provide an efficient and inexpensive method for selective, in situ, real-time chemical sensing.[1−4] The active sensor region of a fiber can be either immobilized at the distal end of an optical fiber (extrinsic)[2,5] or distributed along the length of the fiber-optic waveguide (intrinsic).[6,7] Submicrometer sized extensive fiber-optic sensors have also been reported,[8] and the development of distributed[9] and multiplexed[9,10] fiber-optic sensors is of current interest.

Fiber-optic chemical sensors utilizing evanescent excitation of sensor chromophores have been reported for a variety of inorganic, organic, and biological analytes.[5−7,11−13] For example, electrochromic thin films can be used to monitor residual chlorine,[11] fluorescently labeled antibodies have been used as extrinsic toxin sensors,[5] bare fiber-optic cores (i.e., unclad) have been used to detect dye molecules in solution,[7] and thin polyaniline coatings have been demonstrated as an intrinsic pH sensor.[6] Distributed fiber-optic gas sensors have also been demonstrated utilizing rubbery cladding materials [e.g., poly(dimethyl siloxane)] that permit the diffusion of gases.[12]

A porous glass matrix can both greatly increase the sensor surface area and permit diffusion of analytes into the optical excitation region. For example, chemically etched glass fiber cores (with pore sizes in the range 4−80 nm) have been demonstrated as useful chemical sensors for pH, carbon monoxide, ammonia gas, and moisture detection,[3] however, the porous waveguide greatly increases light scattering losses.[3] Porous glass beads have also been used to covalently link sensor chromophores (e.g., pH-dependent fluorescein derivatives).[14] More recently, sol−gel glass materials have been used as a means of noncovalently incorporating a variety of sensor chromophores into a porous matrix that permits the diffusion of analytes into the

(1) Seitz, W. R. *CRC Crit. Rev. Anal. Chem.* **1988**, *19*, 135−173.
(2) Barnard, S.; Walt, D. *Environ. Sci. Technol.* **1991**, *25*, 1301−1304.
(3) Moslehi, B.; Shahriari, M.; Schmidlin, E.; Anderson, M.; Lukasiewicz, M. *Laser Focus World* **1992**, April, 161−168.
(4) Arnold, M. A. *Anal. Chem.* **1992**, *64*, 1015A−1025A.
(5) Hobbs, J. R. *Laser Focus World* **1992**, May, 83−86.
(6) Ge, Z.; Brown, C. W.; Sun, L.; Yang, S. C. *Anal. Chem.* **1993**, *65*, 2335−2338.
(7) Periasamy, N. *Appl. Opt.* **1982**, *21*, 2693−2695.
(8) Tan, W.; Shi, Z.-Y.; Kopelman, R. *Anal. Chem.* **1992**, *64*, 2985−2990.
(9) SPIE Conference on Optics, Imaging, and Instrumentation, San Diego, CA, July 24−29, 1994 (Symposia: 2292, Fiber Optic and Laser Sensors XII; 2293, Chemical, Biochemical, and Environmental Fiber Sensors VI; 2294, Distributed and Multiplexed Fiber Optic Sensors IV).
(10) Pantano, P.; Walt, D. R. *Anal. Chem.* **1995**, *67*, 481A−487A.
(11) Piraud, C.; Mwarania, E.; Wylangowski, G.; Wilkinson, J.; O'Dwyer, K.; Schiffrin, D. J. *Anal. Chem.* **1992**, *64*, 651−655.
(12) Leiberman, R. A.; Blyler, L. L.; Cohen, L. G. *J. Lightwave Technol.* **1990**, *8*, 212−220.
(13) Lundgren, J. S.; Bekos, E. J.; Wang, R.; Bright, F. V. *Anal. Chem.* **1994**, *66*, 2433−2440.
(14) Fuh, M.-R. S.; Burgess, L. W.; Hirschfeld, T.; Christian, G. D.; Wang, F. *Analyst* **1987**, *112*, 1159−1163.

S0003-2700(96)00078-9 CCC: $12.00 

matrix.[15] A variety of doped sol−gel glasses have been demonstrated as environmental impurity sensors.[16] For example, oxazine-170-doped sol−gel glasses have been demonstrated as a reversible optical sensor for ammonia and acidity,[17] a variety of pH indicators have been doped into sol−gel glasses,[18] and sol−gel glasses have also been shown to be versatile host matrices for active enzyme systems.[19−23] Miniaturized (micrometer-sized) sol−gel-based sensors have also been demonstrated.[24]

A number of sol−gel-based sensors utilizing fiber-optic waveguides have also been reported.[25−28] For example, MacCraith et al.[26] have reported a pH sensor that uses evanescent wave excitation of fluorescein-doped silica cladding at the distal end of a fiber-optic waveguide, and an intrinsic sol−gel-based fiber-optic oxygen sensor has been reported that is based on oxygen quenching of the luminescence of sol−gel-incorporated ruthenium complexes.[27]

Sol−gel chemistry provides a convenient method for incorporating sensor chromophores into porous inorganic glass hosts, from which thin films and coatings can be produced by dip-coating or spin-casting.[29−31] The chemical synthesis of xerogel glasses results in an optically clear, porous glass, with a low index of refraction, and the ability to solvate many different sensor chromophores. The unique chemistry and the porous nature of the xerogel matrix make it well suited to novel optical sensor applications.[15,20,26−28]

In the present study, we demonstrate a simplified pulsed excitation and time-resolved detection technique for monitoring intrinsic sol−gel clad sensors distributed along a fiber-optic waveguide. Time-resolved detection allows simultaneous probing of a distribution of multiplexed sensor regions along a single fiber-optic waveguide. Pulsed evanescent excitation with time-resolved emission detection can be used to spatially resolve individual sensor regions distributed along the fiber-optic waveguide. Furthermore, changes in the emission kinetics provide an additional sensor mechanism that is independent of the chromophore concentration and that may not be accompanied by significant spectral changes.[32]

Although modulated (e.g., ∼100 MHz) evanescent excitation combined with phased resolved fluorescence detection can be used to resolve multiple chromophores doped into a sol−gel matrix,[13] the time-resolved fluorescence detection method presented in this study provides a simple method for simultaneously monitoring the spectral changes, spatial location, and kinetic changes associated with a distribution of separate intrinsic fiber-optic sensor regions.

## SOL−GEL CLAD FIBER OPTICS

**Coupling the Evanescent Wave to Sol−Gel Cladding.** A fiber-optic waveguide is characterized by total internal reflection within the fiber core. However, the evanescent field intensity that extends into the cladding region can be used to optically excite chromophores doped into the cladding.[1] The intensity of the evanescent field drops exponentially with distance away from the core/cladding surface as[33]

$$I(z) = I_o \exp(-z/d_p) \quad (1)$$

where $z$ is the distance outside the cladding/core interface, $I_o$ is the light intensity at the cladding/core boundary, and $d_p$ is the penetration depth for an angle of incidence $\theta$ (greater than the critical angle), given by[33]

$$d_p \frac{\lambda_o}{4\pi}(n_1^2 \sin^2 \theta - n_2^2)^{-1/2} \quad (2)$$

where $\lambda_o$ is the vacuum wavelength and $n_1$ and $n_2$ are the refractive indexes of the core and the cladding material, respectively. Since the propagation direction of the light is nearly collinear with the fiber (i.e., $\theta \approx 90°$), $d_p \approx \lambda_o/(4\pi n_2)$, produces significant evanescent intensity 1 $\mu$m away from the core. Thus, fluorophore molecules situated within this distance can be optically excited and can couple a significant fraction of their emission intensity back into the fiber.

**Distributed Intrinsic Sensors: Spatial Resolution by Time-Resolved Detection.** Time-resolved fluorescent detection following pulsed excitation can be used to probe distributed intrinsic fiber-optic sensors, resolve fluorophore locations along the fiber, and yield the optical dynamics of the chromophore. The spatial resolution of this technique is ultimately determined by the fluorophore lifetime, resulting in a typical spatial resolution of <10 cm.

The distance from the fiber front to a fluorophore-doped sol−gel clad region is given by

$$x = (c/2n)\tau_d \quad (3)$$

where $c$ is the speed of light in the fiber, $n$ is the index of refraction of the silica core, and $\tau_d$ is the time delay between the excitation pulse entering and the emission pulse exiting the fiber front. By measuring the time delay between the excitation pulse reflected from the fiber front and the subsequent fluorescence emission from each sensor region, the distance to each sensor location may be determined. This provides a simple manner for distinguishing


(15) Lev, O.; Tsionsky, M.; Rabinovich, L.; Glezer, V.; Sampath, S.; Pankratov, I.; Gun, J. *Anal. Chem.* **1995**, *67*, 22A−30A.
(16) Reisfeld, R. In Sol−Gel Optics; MacKenzie, J. D., Ulrich, D., Eds.; Proceedings of SPIE 1328; SPIE: Bellingham, WA, 1990; pp 29−39.
(17) Reisfeld, R. *J. Non-Cryst. Solids* **1990**, *121*, 254−266.
(18) Avnir, D. *Acc. Chem. Res.* **1995**, *28*, 328−334.
(19) Dunn, B.; Valentine, J. S.; Zink, J. I. *Science* **1992**, *257*, 147−148.
(20) Dave, B.; Dunn, B.; Valentine, J. S.; Zink, J. I. *Anal. Chem.* **1994**, *66*, 1120A−1127A.
(21) Braun, S.; Rappoport, S.; Zusman, R.; Avnir, D.; Ottolenghi, M. *Mater. Lett.* **1990**, *10*, 1−5.
(22) Wu, S.; Ellerby, L.; Cohan, J.; Dunn, B.; El-Sayed, M.; Valentine, J.; Zink, J. I. *Chem. Mater.* **1993**, *5*, 115−120.
(23) Ellerby, L.; Nishida, C.; Nishida, P.; Yamanaka, S.; Dunn, B.; Valentine, J.; Zink, J. I. *Science* **1992**, *255*, 1113−1115.
(24) Samuel, J.; Strinkovski, A.; Shalom, S.; Lieberman, K.; Ottolenghi, M.; Avnir, D.; Lewis, A. *Mater. Lett.* **1994**, *21*, 431−434.
(25) Grattan, K. T. V.; Badini, G. E.; Palmer, A. W.; Tseung, A. C. C. *Sens. Actuators* **1991**, *A26*, 483−487.
(26) MacCraith, B. D.; Ruddy, V.; Potter, C.; O'Kelly, B.; McGilp, J. F. *Electron. Lett.* **1991**, *27*, 1247−1248.
(27) MacCraith, B. D.; McDonagh, C. M.; O'Keefe, G.; Keyes, E. T.; Vos, J. G.; O'Kelly, B.; McGilp, J. F. *Analyst* **1993**, *118*, 385−388.
(28) MacCraith, B. D.; McDonagh, C. M.; O'Keefe, G.; McEvoy, A. K.; Butler, T.; Sheridan, F. R. *Sens. Actuators* **1995**, *B29*, 51−57.
(29) Dunn, B.; Knobbe, E.; McKiernan, J. M.; Pouxviel, J. C.; Zink, J. I. In *Better Ceramics Through Chemistry III*; Brinker, C. J., Clark, D. E., Ulrich, D. R., Eds.; MRS Proceedings 121; Materials Research Society: Pittsburgh, PA, 1988; pp 331−342.
(30) Hench, L.; West, J.; Zhu, B.; Ochoa, R. In ref 16, pp 230−240.
(31) Avnir, D.; Kaufman, V.; Reisfeld, R. *J. Non-Cryst. Solids* **1985**, *74*, 395−406. Kaufman, V.; Avnir, D. *Langmuir* **1986**, *2*, 717−722. Avnir, D.; Levy, D.; Reisfeld, R. *J. Phys. Chem.* **1984**, *88*, 5956−5959. Kaufman, V.; Avnir, D.; Pines-Rojanski, D.; Huppert, D. *J. Non-Cryst. Solids* **1988**, *99*, 379−386.
(32) Thompson, R. B.; Lakowicz, J. R. *Anal. Chem.* **1993**, *65*, 853−856.
(33) Yariv, A. *Quantum Electronics*, 3rd ed.; John Wiley & Sons: New York, 1989; pp 640−649.

between different sensor regions of the optical fiber, or alternatively, it can be used to spatially locate a sensor response along a fiber uniformly clad with a particular sol−gel sensor film.

## EXPERIMENTAL SECTION

**Sol−Gel Matrix**. Porous xerogel glass claddings were prepared by the room temperature hydrolysis of metal alkoxide solutions.[34] Both silicate and aluminosilicate xerogel claddings were applied by dip-coating silica core fibers. The silicate coatings are prepared by mixing tetraethoxysilane (TEOS) with an ethanol dye solution and 0.01 N hydrochloric acid in a 3:11:1 volume ratio and mixing in a sonicator for 15 min. By controlling the polymerization pH, the pore size distribution of silica xerogel glasses can be controlled to trap dopant molecules, yet allow solvent diffusion.[34−36] The aluminosilicate coatings are prepared by mixing (di-*sec*-butoxyaluminoxy)triethoxysilane (95%, Petrarch) and a 2-propanol/dye solution in a 2:2 volume ratio. Separately, distilled water and a 2-propanol/dye solution are mixed in a 1:10 volume ratio, and this alcohol/water solution is added dropwise to the first solution during sonication.

A variety of organic sensors/fluorophores can be easily doped into the porous xerogel glass matrix[29−31] by the previous recipes. Cresyl violet 670 perchlorate (CV, Exciton), 9-aminoacridine hydrochloride hemihydrate 98% (AA, Aldrich), and disodium fluorescein (FL, Exciton) were doped into the TEOS solution used to clad the optical fibers. An undoped aluminosilica sol−gel cladding was used to bind quinizarin to form an aluminum complex with distinct spectral properties. No significant changes in the fluorescence properties of the doped sol−gel glasses were observed for aging times of 1−2 months; however, since sol−gel-based sensor materials can evolve with age, the long term stability of sol−gel based sensor/fluorophore systems remains an important device application issue.[37]

**Sol−Gel Clad Fiber**. A sketch of a fiber-optic waveguide with intrinsic sol−gel clad regions is shown in Figure 1. A silicone clad multimode (400 $\mu$m core diameter) silica core fiber-optic waveguide[38] was purchased (General Fiber Optics, Inc.). Multiple small sections (~4 cm long) of the silicone cladding were then removed using a commercial silicone remover (McGean-Rohco, Inc.). After stripping, the bare silica core regions were rinsed with ethanol, a 5% hydrofluoric acid solution, and distilled water. These sections were then coated with a sol−gel film by dip-coating[39] into a dye-doped sol−gel solution. CV, AA, and FL were used as dopants in the sol−gel solutions used to clad the optical fibers. A single dip-coat yielded a cladding thickness of ~1 $\mu$m, and the processes could be repeated to increase the cladding thickness.

**Optical Setup**. The basic components of the experimental setup were chosen with an eye toward minimizing the cost and complexity of the system, with the goal of a portable system. A schematic of the optical setup is shown in Figure 2. A small, nitrogen-pumped dye laser (PTI PL2300/PL201) was utilized as the excitation source, with tunable pulses of energy 100 $\mu$J, pulse width of 0.5 ns, and a 20 Hz repetition rate. The fiber emission was collected in a backscattered direction, passed through an excitation cutoff filter, and detected using a fast photomultiplier tube (Hamamatsu R-1635; rise time of 0.8 ns) and an inexpensive (6-bit) 400 MHz digitizing oscilloscope (HP 54502A; rise time of 0.88 ns), yielding a ~1 ns instrument response time without deconvolution. A 6-bit transient digitizer was chosen to minimize the cost of the overall system; however, this can give rise to significant digitization noise, which can be reduced by acquiring and adding several separate traces. For a more portable (and

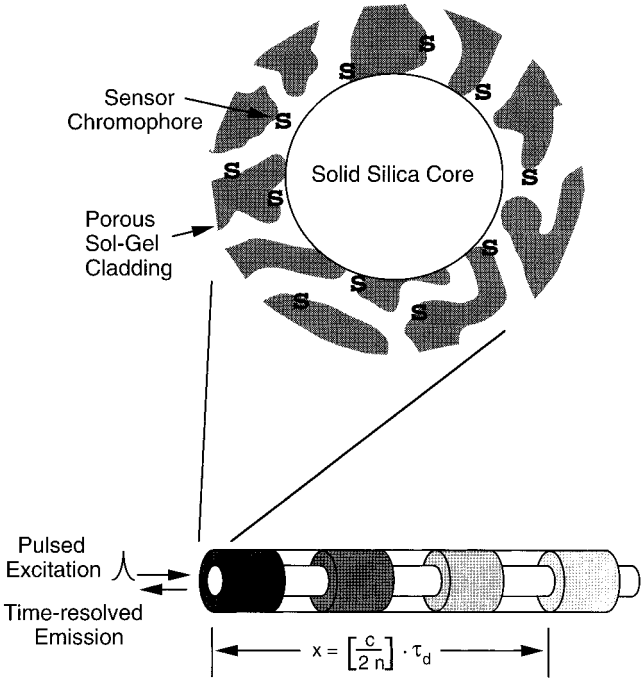


Figure 1. Schematic of a sol−gel clad fiber (not to scale) incorporating sensor molecules (S). The porous matrix and large surface area of the xerogel matrix enhance the number of sensor molecules within the evanescent wave region and allow diffusion of analytes into this region. The fibers utilized in this study consisted of a solid silica core (400 $\mu$m diameter) with a silicone cladding (50 $\mu$m thick) that was locally replaced with fluorophore-doped sol−gel clad regions. The ability to spatially resolve the sensor response using pulsed excitation and time-resolved emission detection using eq 3 is also indicated.

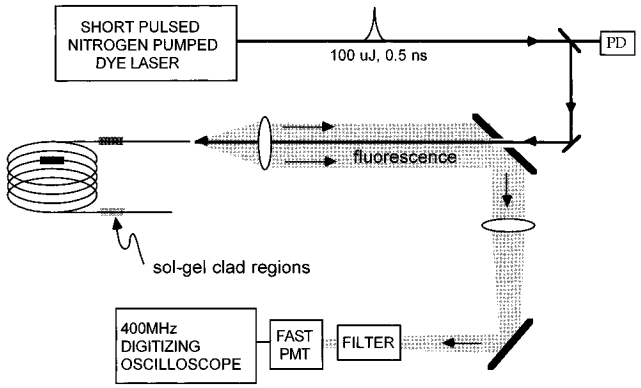


Figure 2. Basic experimental arrangement consisting of a pulsed tunable light source ($N_2$-pumped dye laser); a few mirrors, lenses, and optical filters; a fast PMT detector; and a 6-bit 400 MHz digitizing oscilloscope.


(34) McKiernan, J.; Pouxviel, J.-C.; Dunn, B.; Zink, J. *J. Phys. Chem.* **1989**, *93*, 2129−2133.

(35) Aharonson, N.; Altstein, M.; Avidan, G.; Avnir, D.; Bronshtein, A.; Lewis, A.; Liberman, K.; Ottolenghi, M.; Polevaya, Y.; Rottman, C.; Samuel, J.; Shalom, S.; Strinkovski, A.; Turniansky, A. In *Better Ceramics Through Chemistry VI*; Cheetham, A., Brinker, C., MeCartney, M., Sanchez, C., Eds.; MRS Proceedings 346; Materials Research Society: Pittsburgh, PA, 1994; pp 519−530.

(36) Yamane, M.; Aso, S.; Sakaino, T. *J. Mater. Sci.* **1978**, *13*, 865−870.

(37) Dunbar, R.; Jordan, J. D.; Bright, F. V. *Anal. Chem.* **1996**, *68*, 604−610.

(38) Martinelli, V. *Laser Focus World* **1994**, July, 62−69.

(39) Dislich, H. *J. Non-Cryst. Solids* **1983**, *57*, 371−388.

even less expensive) system, a pulsed diode laser-based excitation source could be utilized.

## RESULTS AND DISCUSSION

Below, we discuss the use of pulsed excitation and time-resolved detection to obtain both spatial resolution and fluorophore kinetics. Also, narrow band excitation and spectrally resolved emission are utilized as additional means of addressing individual intrinsic fluorophore-doped sol−gel clad regions distributed along an optical fiber. Finally, we demonstrate time-resolved detection of intrinsic distributed sol−gel clad fiber-optic sensors.

**Time-Resolved Optical Detection. (a) Simultaneous Detection of Distributed Chromophores.** The time-resolved emission from a distribution of intrinsic sol−gel clad regions along a single optical fiber can be used to independently detect the emission of each cladding element, even in situations where spectral overlap exists. The emissions of the different fluorophore regions are clearly resolved if the physical distance between these regions, $\Delta x$, is larger than the product of the fluorophore emission lifetime and the speed of light in the fiber core. For example, a 1 ns fluorescence lifetime and an index of refraction of $n = 1.5$ yield an optimal sensor spacing of ≥20 cm. Furthermore, optical fiber-based fluorescence lifetime measurement techniques[40] have been extended to simultaneously measure the fluorescence lifetimes of several intrinsic fluorophores distributed along a single optical fiber (Fluorophore Lifetimes, below).

**(b) Spatial Resolution.** Fiber-optic sensor bundles can be used to obtain microscopic spatial resolution at the distal end of the fiber.[10] In contrast, a focus of the present study is the investigation of intrinsic chemical sensors macroscopically distributed along a single optical fiber, e.g., suitable for environmental sensing applications.[41−43] The temporal delay between optical excitation and emission detection of different fluorophore elements is simply related to the distance light must travel in the fiber core and the index of refraction of the fiber core, as given in eq 3. To demonstrate the optical response of sol−gel clad fluorophores, AA and CV dyes were incorporated into intrinsic regions distributed along a single fiber-optic waveguide. A fiber consisting of two bands doped with AA and two others doped with CV is sketched in Figure 3, along with the corresponding time-resolved emission following pulsed excitation of this fiber. The well-resolved CV and AA emission pulses illustrate the ability to monitor a distribution of multiplexed fluorophores along a single optical fiber.

When an excitation pulse wavelength of $\lambda = 424$ nm was used to simultaneously excite both the CV- and AA-doped sol−gel clad regions along a silica core optical fiber, we obtained the upper time-resolved emission trace shown in Figure 3. Fluorescence emissions from all four of the doped sol−gel clad bands are clearly resolved. The reflected signal from the fiber input face provides a convenient reference point for calibrating the subsequent fluorescence emission from the CV- and AA-doped sol−gel clad fiber regions. The time delay of the different emission pulses correlates with the spatial locations of the corresponding fluorophore-doped sol−gel clad regions along the fiber, as given by eq 3 (e.g., ∼5 ft separation between each band). The different relative intensities from the different sol−gel regions result from fiber propagation losses and variations in cladding thickness and were not a focus of this study.

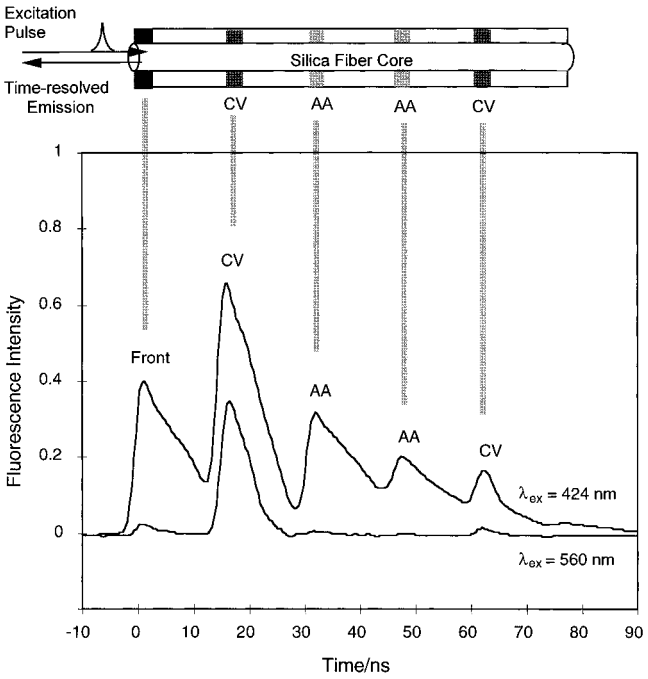


Figure 3. (Above) Schematic of the spatial location of intrinsic chromophore-doped sol−gel clad regions along an optical fiber. The corresponding time-resolved emission following pulsed laser excitation of the sol−gel clad fiber-optic wavequide is also shown. The vertical lines correlate the different emission signals with the corresponding fiber cladding regions. The upper trace was obtained with an excitation wavelength of 424 nm and detection of all emission ≥475 nm. In the lower trace, the time-resolved emission intensity from the AA chromophores was selectively reduced by shifting the excitation wavelength to the red of the AA absorption (e.g., $\lambda_{ex} = 560$ nm).

**(c) Fluorophore Lifetimes**. It is straightforward to extend fiber-optic fluorescence lifetime techniques[40] to obtain simultaneous fluorescence lifetime measurements on several intrinsic sol−gel clad fluorophores. The temporal profile of each individual emission band is characteristic of the fluorescence lifetimes of the corresponding fluorophore. Since both the 0.5 ns excitation pulse and the optical transit time across a 4 cm wide sensor element (0.13 ns) are short relative to the fluorescence lifetimes of the chromophores in this study, the time-resolved emission can be used to probe the emission kinetics of the fluorophores, as shown in Figure 4. The smooth curve in Figure 4 is a least-squares fit of a sum of exponential decays (with appropriate time offsets corresponding to the spatial locations of the fluorophore bands along the fiber). The least-squares fit yields values of 11.5 ± 0.5 ns for the AA fluorescence bands and 3.5 ± 0.4 ns for the last CV emission band (95% confidence limits). The point should be stressed that the goal of the measurement in Figure 4 was simply to detect and correlate emission maxima with the location of doped sol−gel clad regions; i.e., no attempt was made to optimize the conditions for measuring fluorescence lifetimes. Nevertheless, even this relatively crude measurement could differentiate and identify fluorophores on the basis of their emission kinetics. Improved kinetic resolution can easily be obtained by adding several traces together to alleviate the 6-bit

(40) Brown, R. S.; Brennan, J. D.; Krull, U. J. *Microchem. J.* **1994**, *50*, 337−350.
(41) Kersey, A. D. *Distributed and Multiplexed Fiber Optic Sensors II*; Proceedings of SPIE 1797; SPIE: Bellingham, WA, 1992; pp 161−185.
(42) Dakin, J. P. In ref 41, pp 76−108.
(43) Tabacco, M.; Zhou, Q.; Nelson, B. *Chemical, Biochemical, and Environmental Fiber Sensors III*; Proceedings of SPIE 1587; SPIE: Bellingham, WA, 1991; pp 271−277.

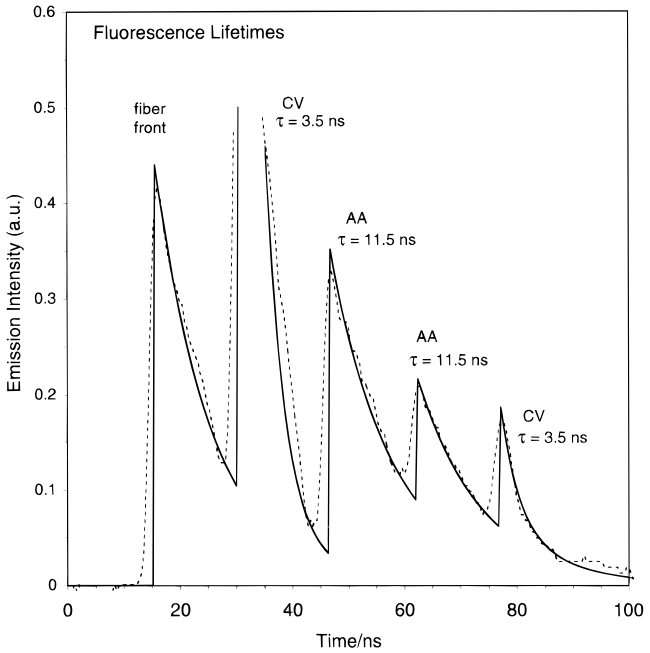


Figure 4. Time-resolved emission from aminoacridine (AA)- and cresyl violet (CV)-doped sol−gel clad regions distributed along a 9 m long fiber-optic waveguide (dashed curve). The solid curve is a least-squares fit of the data to a sum of time-offset exponential decays (corresponding to the locations of the fluorophore bands along the fiber). This fit yields values of 3.5 ± 0.4 ns for the CV emission bands and 11.5 ± 0.5 ns for the AA emission bands.

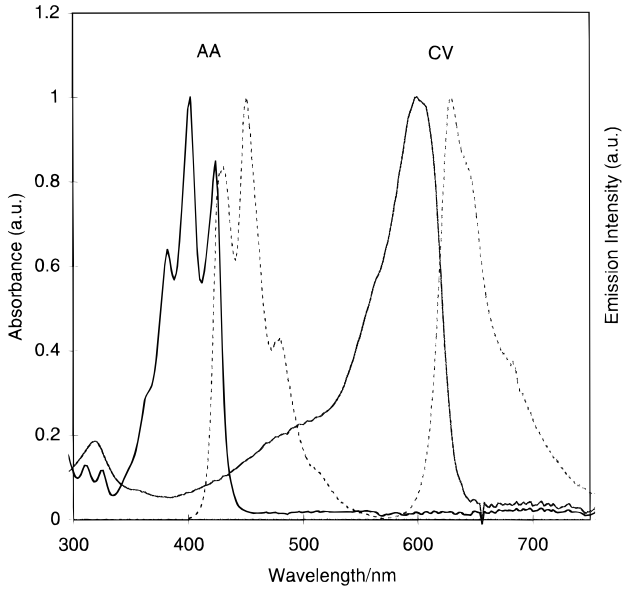


Figure 5. Absorption (solid line) and emission (dotted line) spectra of aminoacridine (AA) and cresyl violet (CV). The well-resolved absorption and emission bands of these two chromophores facilitate selective excitation and/or emission from different sol−gel clad regions along the fiber-optic waveguide, as illustrated in Figure 3.

dynamic range of the transient digitizer, by acquiring several traces on different digitizer voltage scales to minimize saturation and to utilize the full dynamic range for emission bands of varying intensity, and by spatially separating the sol−gel clad regions to reduced band congestion and optical reflections.

The ability to resolve the fluorophore decay kinetics of a distributed array of intrinsic chromophore regions along the fiber-optic indicates that changes in fluorescence kinetics may be used as an additional variable for detecting the individual responses of a distribution of intrinsic sensors.[1,32] A sensor device based upon kinetic changes can alleviate sensor degradation and leaching problems, since the emission lifetime is insensitive to chromophore concentration.

**Spectral Resolution.** Selective optical excitation and detection of an integrated array of sensor elements can be obtained utilizing tunable narrow band excitation combined with spectrally and temporally resolved emission of multiple chromophore elements. To illustrate this, a $\lambda = 424$ nm excitation pulse is used to simultaneously excite CV- and AA-doped sol−gel clad regions along a silica core optical fiber, as indicated by the upper time-resolved emission trace shown in Figure 3. Fluorescence emissions from all four of the chromophore-doped cladding bands are observed since the photon energy of the excitation pulse is sufficient to excite both the AA and the CV chromophores.

The CV and AA absorption bands shown in Figure 5 indicate that longer wavelength excitation (e.g., $\lambda = 590$ nm) can be used to preferentially excite only the CV-doped sol−gel clad regions, as shown in the lower trace in Figure 3. In addition, spectral filtering of the emission can also be used to discriminate between AA and CV emission due to the well-resolved emission bands, also shown in Figure 5. For example, even when both the AA and CV chromophores are excited, a $\lambda \geq 560$ nm emission cutoff filter transmits only the redder CV emission (not shown), resulting in an emission trace similar to the lower trace in Figure 3.

**Intrinsic Sol−Gel Clad Fiber-Optic Sensors.** In the following sections, time-resolved optical detection of prototypical sol−gel clad fiber-optic sensor waveguides is demonstrated. The porous nature of the xerogel allows diffusion of analyte species into the evanescent field region of the cladding, where they can be optically detected. A FL-doped silica xerogel clad fiber and an undoped aluminosilica xerogel clad fiber are demonstrated as intrinsic pH and quinone sensors, respectively.

**(a) pH Sensor.** The absorption maximum of FL in a porous silica xerogel (SX) shifts from 490 nm in a pH = 7 solution to 440 nm when immersed in a pH = 2 solution, as shown in Figure 6a. The origins of the pH-induced spectral shifts observed for fluorescein in solution and in sol−gel matrices are discussed in ref 44 and 45, respectively. The large pH-induced change in the FL absorption spectrum indicates that protons (and associated ions) are able to easily diffuse through the porous xerogel matrix. A 7 m long fiber with a single FL-doped sol−gel clad region was utilized as a prototypical intrinsic optical fiber pH sensor. Using an excitation wavelength of 500 nm, the emission intensity from the FL-doped sol−gel clad region was observed to decrease as the pH of the solution surrounding the cladding region was lowered, as shown in Figure 7a. At lower pH, the FL/SX absorbance at 500 nm is reduced (as shown in Figure 6a), resulting in a corresponding decrease in emission intensity. Reflections of the excitation pulse off of both the front and the distal ends of the 7 m long fiber are useful reference points. In between every new pH measurement, a control measurement at pH = 7 was taken to ensure that cladding degradation and/or laser fluctuations were not responsible for the observed changes. The intensity of these control measurements (not shown) varied

(44) Fuji, T.; Ishii, A.; Kurihara, Y.; Anpo, M. *Res. Chem. Intermed.* **1993**, *19*, 333−342.
(45) Shamansky, L. M.; Yang, M.; Olteanu, M.; Chronister, E. L. *Mater. Lett.* **1996**, *26*, 113−119.

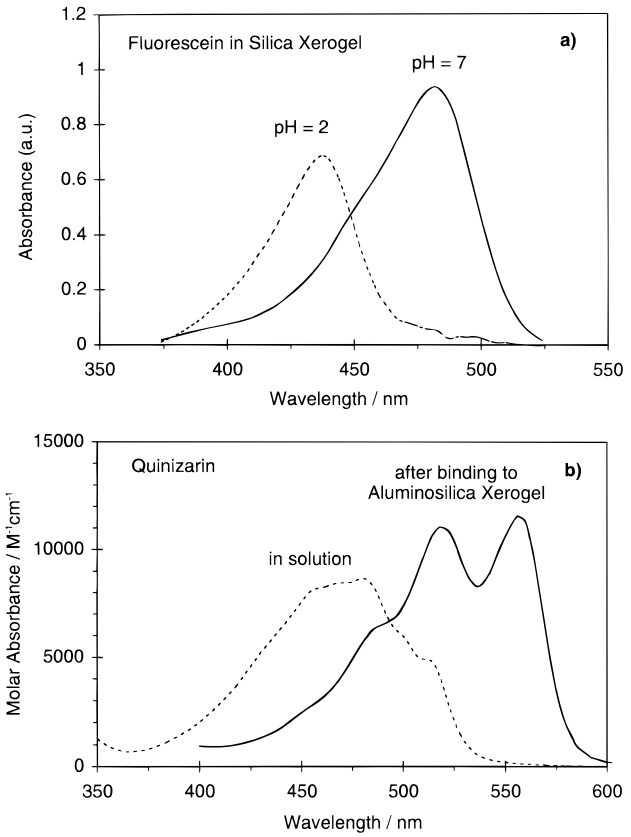


Figure 6. (a) Absorption spectrum of fluorescein in a silica xerogel immersed in two different pH solutions of pH = 2 (dashed curve) and pH = 7 (solid curve).[45] The 500 nm excitation wavelength used in Figure 7 is more strongly absorbed by the high pH form of FL. (b) Quinizarin absorption spectrum, which shifts to the red upon complexation with aluminum in the ASX matrix. The 560 nm excitation wavelength used in Figure 8 is more strongly absorbed by the Q−Al complex formed as Q binds to the ASX cladding.

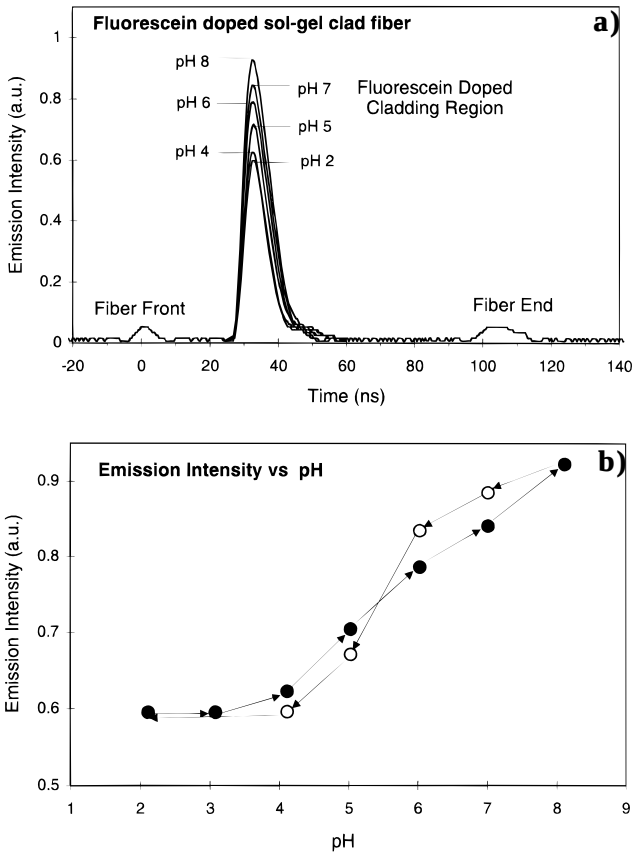


Figure 7. (a) Time-resolved emission intensity following pulsed evanescent excitation (at $\lambda_{ex}$ = 500 nm) of an intrinsic fluorescein-doped sol−gel clad region on a 7 m long fiber-optic waveguide. Since 500 nm is near the absorption maximum of the high-pH form of fluorescein (as shown in Figure 6a), a decrease in absorption (and emission) is observed as the pH is lowered. The arrows indicate the order in which the different pH measurements were performed. Reflections of the excitation pulse off of both the front and the distal ends of the 7 m long fiber are shown for reference. (b) The results from part a yield a pH titration curve for the time-resolved fiber-optic sensor. The arrows indicate the order in which the pH changes were made, except for pH = 7 control measurements (not shown), which were taken between each pH change.

by only ±4% over the six pH measurements, demonstrating the reversibility of the pH sensor. Furthermore, the titration of the time-resolved sensor emission intensity, shown in Figure 7b, is similar to static spectroscopic studies of FL in solution and doped into SX monoliths.[45]

**(b) Quinone Sensor.** The pores of the sol−gel matrix are large enough to allow the diffusion of larger organic analytes into the evanescent detection region. An aluminosilica xerogel (ASX) clad region of a fiber-optic waveguide was exposed to a $10^{-3}$ M quinizarin (Q) solution, allowing Q to diffuse into the ASX cladding and irreversibly bind to aluminum in the matrix, forming a Q−Al complex with a distinct spectral signature. The complexation of Q by the ASX matrix can be spectroscopically monitored using the absorption origin of the Q absorption spectrum, which shifts from a wavelength of 520 to 560 nm upon complexation with Al within the ASX matrix,[46,47] as shown in Figure 6b. The time-resolved emission trace shown in Figure 8 was obtained using 560 nm excitation to probe for the formation of the Q−Al complex following exposure of an ASX clad region to a $10^{-3}$ M Q solution. The increase in emission intensity with Q uptake is due to the increased absorption of the Q−Al complex at the excitation wavelength. Since the Q chromophore binds irreversibly, the ASX matrix continues to bind more Q until the accessible sites of the matrix are saturated. It is difficult to quantify the sensitivity of this irreversible sensor, since the signal intensity is more a function of the absolute number of Q molecules in solution (versus the Q concentration). For example, an ASX sample immersed in a large volume of a dilute Q solution can eventually bind more Q compared to a smaller volume of a more concentrated solution.

The response time for binding of Q by the ASX matrix can be complex due to competing factors such as diffusion of Q through solution, diffusion of Q through the pores of the ASX matrix, binding of Q by the ASX matrix, and saturation of the accessible binding sites. Due to the size of the Q analyte, the time necessary for Q to diffuse into the evanescent region of the sol−gel cladding may be significant. Although 30 min was needed to obtain a saturated maximum intensity, a significant signal (∼25% of maximum) was obtained almost instantaneously (∼1 s). The dotted trace in Figure 8 shows the appearance of a second Q−Al emission band following exposure of a second intrinsic ASX band to a $10^{-3}$ M Q solution.

(46) Allen, N.; Hayes, G.; Riley, P.; Richards, A. *J. Photochem.* **1987**, *38*, 365−373.
(47) Basché, Th.; Bräuchle, C. *J. Phys. Chem.* **1991**, *95*, 7130−7131.

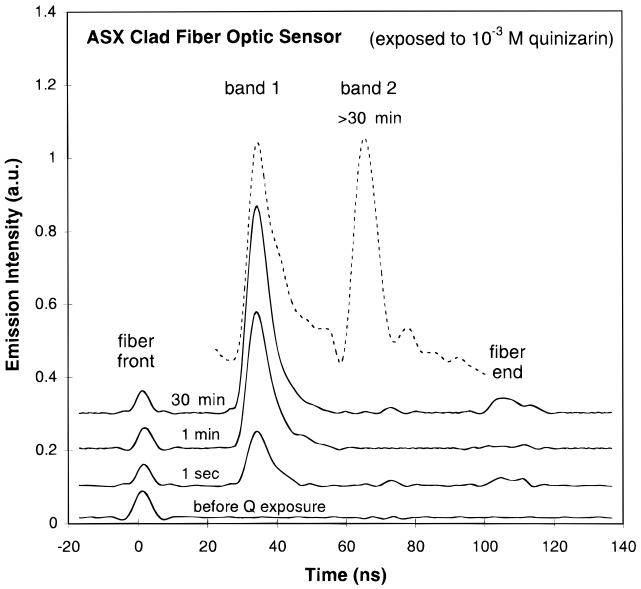


Figure 8. Results of using an excitation wavelength of 560 nm to detect the presence of quinizarin in a $10^{-3}$ M solution surrounding an ASX clad region of a fiber-optic waveguide. As quinizarin diffuses into the ASX cladding, it binds to form a Q−Al complex, which is detected by an increase in the absorbance at 560 nm, with a corresponding increase in the emission intensity from the Q−Al fluorophore. Due to the size of the Q analyte, there is a response time for Q to diffuse into the evanescent region of the sol−gel cladding. The dotted trace shows the result following the subsequent exposure of a second intrinsic ASX band on the same fiber to the $10^{-3}$ M quinizarin solution.

## CONCLUSIONS

Pulsed evanescent excitation and time-resolved detection have been demonstrated as a technique to simultaneously probe intrinsic sol−gel clad sensor elements distributed along a single fiber-optic waveguide. In addition, the temporal delay associated with each emission band is used to spatially resolve the intrinsic fluorophore regions along the fiber. Time-resolved emission has also been used to resolve the emission kinetics for an array of intrinsic sol−gel clad fluorophore regions along the fiber-optic waveguide. Frequency-selective excitation and/or detection can also be used in conjunction with time-resolved detection to further discriminate or address specific sol−gel clad regions. A fluorescein- doped silica xerogel clad fiber and an undoped aluminosilica xerogel clad fiber have been demonstrated as intrinsic pH and quinone sensors, respectively.

## ACKNOWLEDGMENT

This research was supported by an Army Research Office Grant (DAAL03-92-G-0399) and by a U.S. Environmental Protection Agency Grant (R821325-01-0).

Received for review January 29, 1996. Accepted April 24, 1996.[⊗]

AC960078R

[⊗] Abstract published in *Advance ACS Abstracts,* June 1, 1996.